Korean J. Chem. Eng., **29**(11), 1567-1576 (2012)
DOI: 10.1007/s11814-012-0049-5

Biosorption of hazardous textile dyes from aqueous solutions by hen feathers: Batch and column studies

Sagnik Chakraborty, Shamik Chowdhury†, and Papita Das Saha

Department of Biotechnology, National Institute of Technology-Durgapur, Mahatma Gandhi Avenue, Durgapur 713209, West Bengal, India
(*Received 21 January 2012 • accepted 8 April 2012*)

Abstract−The biosorption potential of hen feathers (HFs) to remove hazardous textile dyes, namely congo red (CR) and crystal violet (CV), from their aqueous solutions was investigated in batch and dynamic flow modes of operation. The effect of biosorption process parameters such as solution pH, initial dye concentration, temperature, feed flow rate and bed height was studied. Biosorption equilibrium data were well described by the Langmuir isotherm model. Kinetic studies at different temperatures showed that the rate of biosorption followed the pseudo second-order kinetics well. A thermodynamic study showed that biosorption of both CR and CV was spontaneous and endothermic. Breakthrough time increased with increase in bed height but decreased with increase in flow rate. The Thomas model showed good agreement with the dynamic flow experimental data. Overall, the results suggest the applicability of HFs as an efficient biosorbent for removal of carcinogenic textile dyes from aqueous media.

Key words: Biosorption, Hen Feathers, Congo Red, Crystal Violet, Thermodynamics, Breakthrough

INTRODUCTION

The contamination of water resources by synthetic dyes is a serious environmental problem, particularly due to their negative ecotoxicological effects and bioaccumulation in wildlife [1-4]. Over 100,000 different commercially available dyes exist and more than 7×10^5 tons of dyestuff are produced worldwide annually [5]. A large number of industries and sectors, such as textile, leather, paper, printing, food, cosmetics, paint, pigments, petroleum, solvent, rubber, plastic, pesticide, wood preserving chemicals and pharmaceutical industry, use dyes to color their products and the effluents of these industries are highly colored [6-8]. The textile manufacturing industry alone discharges about 146,000 tons of dyes per year along with its wastewater which ultimately finds its way into the surrounding water bodies [6].

Increasing concern about the continuing deterioration of the global environment has led to extensive research and development in wastewater treatment processes. Biosorption, defined as the the removal of materials (organic compounds, metal ions, dye molecules etc.) by inactive, non-living biomass (materials of biological origin), has been suggested as an economically viable sustainable technology for the treatment of wastewater streams [9]. A huge number of low-cost biosorbents derived from agricultural/industrial waste such as rice husk [2,6], rice straw [10], groundnut shell [11], tamarind fruit shell [12], wheat shell [13], wheat bran [14], orange peel [15], lemon peel [16], pineapple leaves and stem [9,17], rejected tea [18], deoiled soya [19], fly ash [20], and bottom ash [19] have been investigated intensively for removal of dyes from their aqueous solutions.

Natural materials like feathers (from both chickens and hens) are generated in huge quantities as waste at commercial poultry processing plants. Worldwide, nearly 8.5 billion tons of feathers are generated annually as waste by poultry-processing industries, of which India's contribution alone is 350 million tons [21]. To date, few studies have shown the feasibility of employing feathers as effective and economic biosorbent to remove heavy metals (Cu^{2+}, Pb^{2+}, Ni^{2+}, Cd^{2+}, Hg^{2+}) and dyes (malachite green, tartrazine, brilliant blue FCF and erythrosine) from their aqueous solutions [22-26]. Feathers are composed mainly of keratin, a kind of self organized protein that has interesting physicochemical properties for sorption of organic/inorganic compounds because of the number of functional groups (carboxyl, hydroxyl and amine-groups), both on the backbone and the side chain [22]. Considering this interesting property of feathers, the primary aim of this study was to investigate the possibility of exploiting waste HFs as potential low-cost biosorbent for removal of two synthetic dyes, namely congo red (CR) and crystal violet (CV), from their aqueous solutions. CR is widely used in textiles, paper, rubber and plastic industries [27]. However, the dye can cause allergic reactions and is metabolized to benzidine, a human carcinogen. It is a skin, eye, and gastrointestinal irritant that may also affect blood factors such as clotting, and induce somnolence and respiratory problems [27]. CV is a well known textile colorant [2]. It also finds application in the manufacture of paints and printing inks. The dye is non-biodegradable and environmentally persistent, and has therefore been classified as a recalcitrant molecule [2]. The dye has been found to have cytotoxic and carcinogenic effect on mammalian cells and can also cause severe damage to the cornea and conjunctiva [2]. CR and CV are, respectively, acid and basic dye molecules and therefore release negative and positive charged colored moieties in aqueous solution, allowing the assessment of any preferential surface interaction. Exploitation of the waste feathers for biosorption is a novel approach, solving the problem of waste disposal.

A literature survey shows that most of the studies on dye bio-

†To whom correspondence should be addressed.
E-mail: chowdhuryshamik@gmail.com

sorption using low-cost biosorbents have focused on sorption experiments using batch configurations. Although the sorbent behavior obtained from kinetic and equilibrium studies in batch conditions is useful for the design of a specific sorbate/sorbent system, this data may not be applicable to other, more realistic treatment configurations (e.g., packed bed columns). Studies on packed bed columns is necessary for the design of continuous-flow sorption processes, which allow a more efficient utilization of the sorbent and provide a better quality effluent. Therefore, in this paper we report the removal of CR and CV from their aqueous solutions using HFs in both batch and dynamic flow conditions. Specifically, we report the fundamental biosorption behavior of HFs for removal of CR and CV, including the effect of pH, temperature and initial dye concentration, biosorption isotherms, kinetics and thermodynamics, and continuous column biosorption performance with special focus on the influence of feed flow rate and bed height.

MATERIALS AND METHODS

1. Biosorbent Collection and Preparation

Hen feathers used in this study were collected from a local poultry in Durgapur, West Bengal, India. The feathers were first washed with detergent and rinsed thoroughly with distilled water to remove adhering dirt and any unwanted particles. They were then washed with aqueous ethanol (20% v/v) to remove organic residues, and then rinsed again with distilled water. The washed feathers were then air dried and the barbs were cut into about 0.5 cm length with scissors, discarding the hard middle rachis. This biosorbent size is adequate for performing both batch and continuous experiments and, in particular, is useful to prevent a significant pressure drop during operation of packed bed columns as reported earlier [22]. Finally, the prepared biosorbent was stored in sterile, air tight glass bottles and used without any further treatment for dye biosorption.

2. Dye Solutions

CR (CI 22120, MF: $C_{32}H_{22}N_6Na_2O_6S_2$, FW: 696.7, λ_{max}: 570 nm) and CV (CI 42555, MF: $C_{25}H_{30}N_3Cl$, MW: 408, λ_{max}: 580 nm) used in this study were of commercial grade and used as such without further purification. Dye stock solution (500 mg L^{-1}) was prepared by dissolving accurately weighed quantity of the dye in double distilled water. Experimental solutions of different concentration were prepared by diluting the stock solution with suitable volume of double distilled water. The initial solution pH was adjusted with 0.1 M HCl and 0.1 M NaOH solutions using a digital pH meter (LI 127, ELICO, India) calibrated with standard buffer solutions.

3. Biosorbent Characterization

The surface structure of the biosorbent before and after dye biosorption was analyzed by a scanning electron microscope (S-3000N, Hitachi, Japan) operated at an electron acceleration voltage of 15 kV. Prior to scanning, the unloaded and dye-loaded HF samples were mounted on a stainless steel stab with double stick tape and coated with a thin layer of gold in a high vacuum condition.

4. Batch Biosorption Studies

Batch biosorption experiments were conducted in 250 mL glass-stoppered, Erlenmeyer flasks with 100 mL of dye solution (of desired concentration and pH). A weighed amount (0.5 g) of biosorbent was added to the solution. The flasks were agitated at a constant speed of 150 rpm in an incubator shaker (Innova 42, New Brunswick Scientific, Canada) at a constant temperature of 303±1 K (unless otherwise mentioned) until reaching equilibrium. Each test lasted for nearly 5 h after which the biosorbent was separated from the solution by centrifugation at 5,000 rpm for 5 min. The residual dye concentration in the supernatant was then analyzed by using a UV/Vis spectrophotometer (U-2800, Hitachi, Japan).

4-1. Effect of pH

The effect of pH on the biosorption capacity was studied in the range of 2-10 in batch experiments already described. The biosorbent dose was fixed at 0.5 g, and the initial dye concentration was 50 mg L^{-1}.

4-2. Effect of Initial Dye Concentration

To investigate the effect of initial dye concentration on the biosorption efficiency, batch experiments were carried out by varying the initial dye concentration from 20 to 100 mg L^{-1}; the biosorbent dose fixed at 0.5 g.

4-3. Effect of Temperature

To study the effect of temperature on the biosorption performance, batch experiments as above described were carried out with temperatures 293, 303 and 313 K, respectively. The biosorbent dose was fixed at 0.5 g while the initial dye concentration was 50 mg L^{-1}.

4-4. Kinetic Studies

Kinetic studies were performed by contacting 100 mL (50 mg L^{-1}) dye solution with 0.50 g HFs in 250 mL glass-stoppered, Erlenmeyer flasks at temperatures in the range of 293 to 313 K. Samples were collected from the flasks at fixed time intervals: 5, 10, 20, 30, 40, 50, 60, 90, 120, 150, 180, 210, 240, 270 and 300 min. The withdrawn samples were centrifuged at 5,000 rpm for 5 min to separate the biosorbent from the solution. The residual dye concentration in the samples was then analyzed by using a UV/Vis spectrophotometer (U-2800, Hitachi, Japan).

5. Calculations

The amount of dye adsorbed per unit biosorbent (mg dye per g biosorbent) was calculated according to a mass balance on the dye concentration using Eq. (1):

$$q_e = \frac{(C_i - C_e)V}{m} \quad (1)$$

where C_i is the initial dye concentration (mg L^{-1}), C_e is the equilibrium dye concentration in solution (mg L^{-1}), V is the volume of the solution (L), and m is the mass of the used biosorbent (g).

The percent removal (%) of dye was calculated using the following equation:

$$\text{Removal}\ (\%) = \frac{C_i - C_e}{C_i} \times 100 \quad (2)$$

6. Continuous Biosorption Studies

Continuous flow biosorption experiments were conducted in a glass column (3 cm internal diameter and 50 cm height) at room temperature. A known quantity of the biosorbent was packed into the glass column. A porous sheet was attached at the bottom of the column to support the biosorbent bed. The top of the bed was covered by a layer of glass beads (1 mm in diameter) to avoid the loss of biosorbent and also to ensure a closely packed arrangement (Fig. 1). To eliminate air bubbles inside the column and ensure a good liquid distribution, a definite volume of distilled water was passed through the column prior to biosorption study. Dye solution of known con-

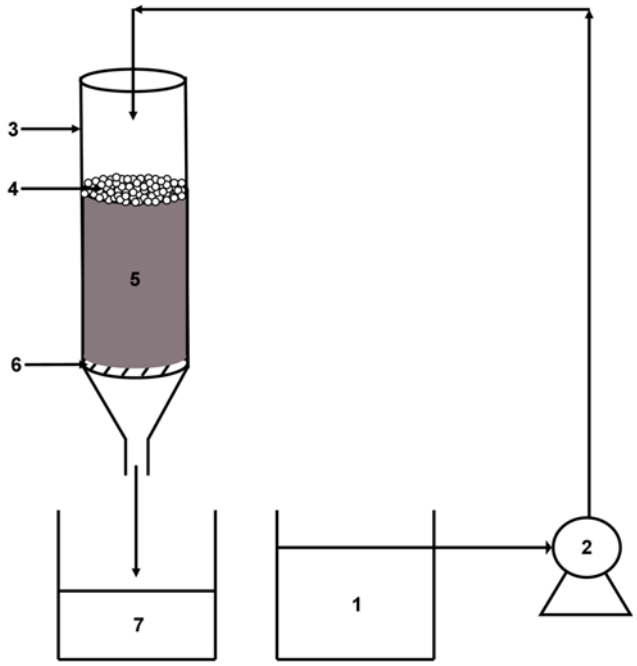

Fig. 1. Schematic diagram of the experimental setup.

1. Feed tank
2. Peristaltic pump
3. Glass column
4. Glass beads
5. HFs
6. Porous sheet
7. Effluent storage tank

centration (50 mg L^{-1}) was pumped to the column in a down-flow direction by a peristaltic pump (PP-EX204C, Miclins, India). The effect of feed flow rate (v) (5-15 mL min^{-1}) and bed height (h) (3-10 cm) was studied. Dye solution at the outlet of the column was collected at regular time intervals and the concentration of the dye in the effluent was analyzed using UV/Vis spectrophotometer (U-2800, Hitachi, Japan). Operation of the column was stopped when the effluent dye concentration exceeded a value of 99.5% of its initial concentration.

7. Statistical Analysis

To ensure the reproducibility of results, all the biosorption experiments were performed in triplicate and the results are presented as means of the replicates along with standard deviation (represented as error bars). Microsoft Excel 2007 program was employed for data processing. Linear regression analysis was used to determine slopes and intercepts of the linear plots and for statistical analysis of the data.

RESULTS AND DISCUSSION

1. Biosorbent Characterization

The SEM micrographs of the biosorbent material before and after dye biosorption are illustrated in Fig. 2(a)-(c). SEM image of the biosorbent material before biosorption shows a main arbor barb with numerous barbules on both sides (Fig. 2(a)). This arrangement indicates a very large surface area that could possibly facilitate the entrapment and subsequent sorption of dye molecules onto the surface of the biosorbent. The morphological characteristic of the biosorbent was altered after dye biosorption. Biosorption of CR induced cracking of the barb (Fig. 2(b)). This could be a consequence of the corrosive nature of the acidic CR dye, thereby facilitating the penetration of the CR molecules within the internal structures of the biosorbent and interact therein with the keratin protein. On the other side, following biosorption of CV there are marked changes on the surface morphology of the biosorbent particularly that of the barbules (Fig. 2(c)). This may be due to possible interaction of CV molecules with the keratin in the barbules.

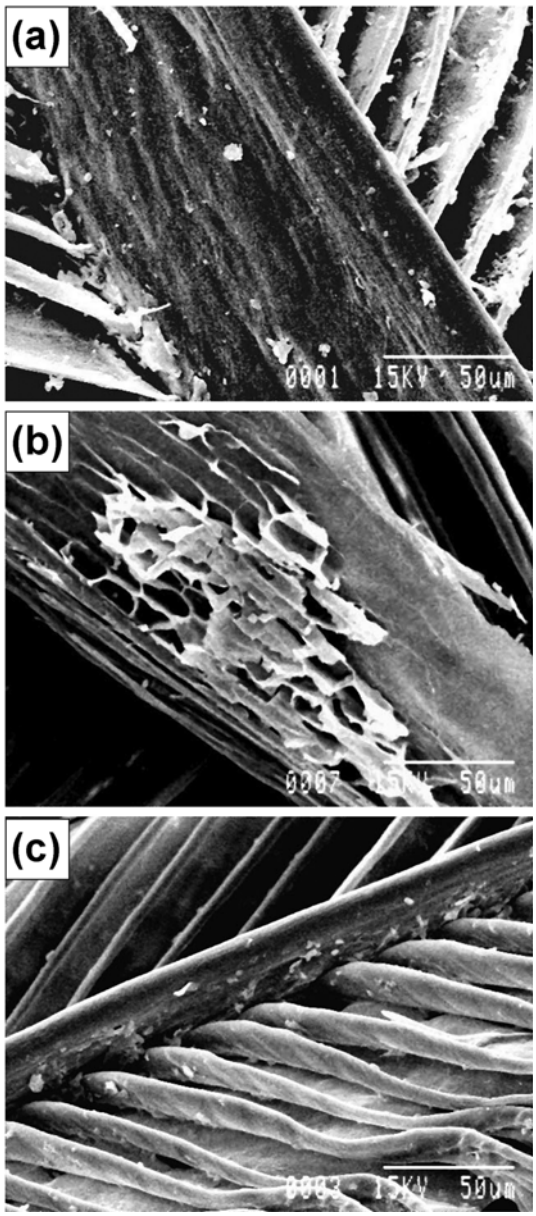

Fig. 2. SEM images of HFs (a) before biosorption (b) after biosorption of CR (c) after biosorption of CV.

2. Batch Studies

2-1. Effect of pH

Solution pH is an important monitoring parameter in dye biosorption processes. It not only influences the surface charge of the biosorbent and the dissociation of functional groups on the active sites of the biosorbent, but also the degree of ionization of the dye present in the solution. Therefore, in the present investigation, the effect of pH on the removal efficiency of CR and CV by HFs was studied at different solution pH ranging from 2.0 to 10.0. Data ob-

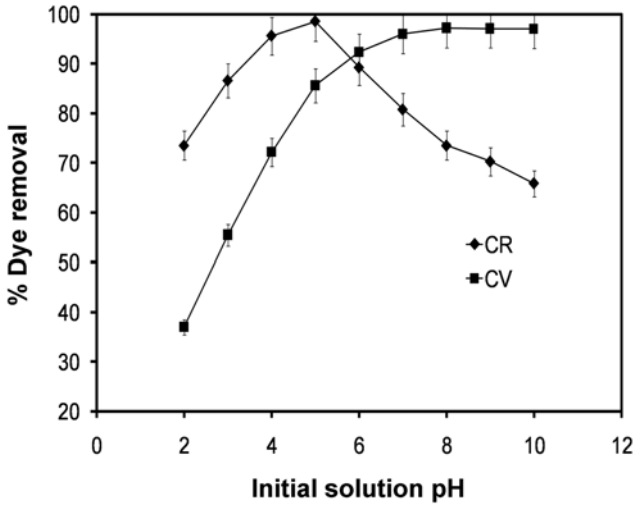

Fig. 3. Effect of pH on biosorption of CR and CV by HFs (experimental conditions: initial dye concentration: 50 mg L^{-1}, biosorbent dose: 0.5 g/0.1 L, agitation speed: 150 rpm, temperature: 303 K, contact time: 5 h).

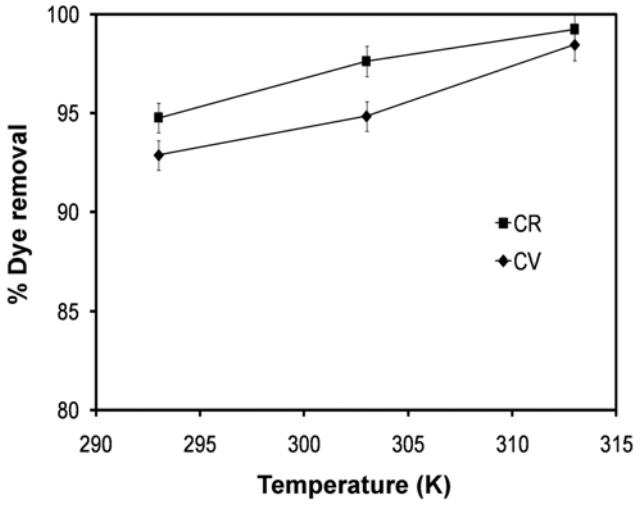

Fig. 4. Effect of temperature on biosorption of CR and CV by HFs (experimental conditions: initial dye concentration: 50 mg L^{-1}, biosorbent dose: 0.5 g/0.1 L, agitation speed: 150 rpm, contact time: 5 h).

tained from the experiments are presented in Fig. 3. Evidently, pH significantly affects the extent of biosorption of both CR and CV by HFs. As seen in Fig. 3, with increase in pH of the solution the percentage removal of CR increases till pH 5.0, but with further increase in pH, percentage removal of dye drops significantly. On the contrary, the percentage removal of CV by HFs increases with increase in solution pH appreciably up to pH 7.0 (Fig. 3). With further increase in pH from 7.0 to 10.0 the percentage CV removal increases, but the difference in the percentage increase is not very significant. The maximum removal of CR and CV was obtained at pH 5.0 and pH 8.0, respectively. Therefore, all further studies pertaining to CR and CV were carried out at pH 5.0 and pH 8.0, respectively.

CR is an anionic dye that exists in aqueous solution in the form of negatively charged ions, while CV is a cationic dye that exists in aqueous solution in the form of positively charged ions. As a charged species, the degree of their biosorption onto the biosorbent surface is primarily influenced by the surface charge of the biosorbent, which in turn is influenced by the solution pH. At low pH values, protonation of the functional groups present on the biosorbent surface easily takes place. The surface of the biosorbent becomes positively charged, and this increases the biosorption of the negatively charged CR ions through electrostatic forces of attraction. However, in case of CV-HFs system, this positive charge density decreases the biosorption of the positively charged CV ions through electrostatic repulsion. With increase in solution pH, deprotonation of the positively charged groups on the biosorbent surface leads to decrease in CR biosorption due to electrostatic repulsion between negatively charged sites on the biosorbent and CR anions. On the other side, the biosorption of CV increases owing to electrostatic attraction between negatively charged sites on the biosorbent and CV cations. The present findings are in accordance with those previously reported for biosorption of CR by neem leaf powder [28] and CV by coniferous pinus bark powder [29].

2-2. Effect of Temperature

Temperature seems to have a great influence on biosorption process, so the effect of temperature on the biosorption of CR and CV by HFs was investigated. Batch biosorption experiments were carried out at different temperatures ranging from 293 to 313 K and the results are shown in Fig. 4. The CR and CV uptake increase with increase in temperature suggesting that CR and CV uptake process were endothermic in nature. An increase in temperature leads to an increase in mobility of the dye molecules. Increasing temperature also decreases the retarding forces acting on the molecules. Therefore, there is an enhancement in the dye binding capacity of the biosorbent with increasing temperature [30]. A quite similar trend has been reported for biosorption of CR by $CaCl_2$ modified bentonite [31] and CV by treated ginger waste [32].

2-3. Effect of Initial Dye Concentration

The effect of different initial dye concentration on the biosorp-

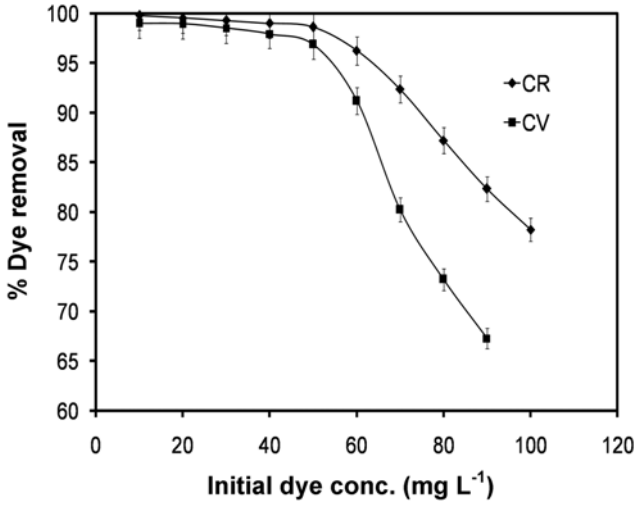

Fig. 5. Effect of initial dye concentration on biosorption of CR and CV by HFs (experimental conditions: biosorbent dose: 0.5 g/0.1 L, agitation speed: 150 rpm, temperature: 303 K, contact time: 5 h).

tion of CR and CV by HFs was also investigated. With increase in initial dye concentration, the dye removal efficiency decreases in both CR-HFs and CV-HFs systems (Fig. 5). This can be explained: all biosorbents have a limited number of active sites, which become saturated at a certain concentration [33]. On the contrary, the amount of dye uptake per unit mass of the biosorbent increases (not shown in Fig. 5). Such behavior is a result of the increase in the driving force from the concentration gradient [33]. In addition, if the concentration of the dye in solution is higher, the active sites of the biosorbent are surrounded by more dye molecules. The biosorption phenomenon occurs more efficiently, and thus the value of q_e increases with the increase of initial dye concentration [34]. Similar results were previously reported for biosorption of CR by clay materials [35] and CV by grapefruit peel waste [36].

2-4. Biosorption Isotherms

In the present investigation, equilibrium data obtained from batch experiments conducted at different temperatures was used for isotherm modeling. The Freundlich, Langmuir and Dubinin-Radushkevich (D-R) isotherm models were used to describe the equilibrium biosorption data of CR and CV [37].

$$\text{Langmuir: } \frac{C_e}{q_e} = \frac{C_e}{q_m} + \frac{1}{K_L q_m} \quad (3)$$

$$\text{Freundlich: } \log q_e = \log K_F + \left(\frac{1}{n}\right)\log C_e \quad (4)$$

$$\text{Dubinin-Radushkevich (D-R): } \ln q_e = \ln q_m - \beta\varepsilon^2 \quad (5)$$

The parameters and correlation coefficients obtained from the plots of Langmuir (C_e/q_e versus C_e), Freundlich ($\log q_e$ versus $\log C_e$) and D-R ($\ln q_e$ versus ε^2) (figures not shown) for both CR and CV are listed in Table 1. Based on the correlation coefficients, the applicability of the isotherms was compared (Table 1). As seen in Table 1, the biosorption of both CR and CV onto HFs follows the Langmuir isotherm model, confirmed by the high values of the correlation coefficients. The excellent fit of the Langmuir isotherm to the experimental biosorption data confirms that the biosorption of both the dyes is monolayer; biosorption of each molecule has equal activation energy, and that sorbate-sorbate interaction is negligible. The maximum biosorption capacity of HFs (q_m) increases from 72.17 mg g^{-1} at 293 K to 78.62 mg g^{-1} at 313 K for CR, while it increases from 55.23 mg g^{-1} at 293 K to 63.49 mg g^{-1} at 313 K for CV. From Table 1, it is also evident that the Langmuir constant, K_L increases with increase in temperature for both the dyes. Seen overall, the information thus obtained specifies an endothermic nature of the existing biosorption processes. The magnitude of the Freundlich constant n gives a measure of favorability of biosorption. The values of n between 1 and 10 (i.e., 1/n less than 1) represent a favorable biosorption process [9]. For the present study the value of n also presents the same trend for both the dyes representing beneficial biosorption processes of CR and CV onto HFs.

To determine the nature of biosorption processes as physical or chemical, the equilibrium biosorption data of CR and CV were also tested with the D-R model. The mean free energy E (kJ mol^{-1}) of biosorption calculated from the D-R isotherm model constant β can characterize the type of biosorption process as chemical ion exchange (E=8-16 kJ mol^{-1}), or physical sorption (E<8 kJ mol^{-1}). E can be calculated using the relationship [2]:

$$E = \frac{1}{\sqrt{2\beta}} \quad (6)$$

The calculated E values were found to be >8 kJ mol^{-1} for both the dyes at all temperatures (Table 1), which implies that biosorption of both CR and CV onto HFs proceeds via a chemical ion exchange mechanism [2,9].

2-5. Biosorption Kinetics

For evaluating the biosorption kinetics of CR and CV onto HFs, the pseudo-first-order and pseudo-second-order kinetic models were fit to the experimental data [37].

$$\text{Pseudo-first-order: } \log(q_e - q_t) = \log q_e - \frac{k_1}{2.303}t \quad (7)$$

$$\text{Pseudo-second-order: } \frac{t}{q_t} = \frac{1}{k_2 q_e^2} + \frac{1}{q_e}t \quad (8)$$

The values of pseudo-first-order rate constants, k_1 and q_e were calculated from the slope and intercept of the plots of $\log(q_e - q_t)$ versus t (figure not shown). The k_1 values, the correlation coefficients, and theoretical and experimental equilibrium biosorption capacity q_e for both the dyes are listed in Table 2. The low correlation coefficient values at all temperatures for both CR and CV suggest that the pseudo-first-order kinetic model was not suitable for describing the kinetics of the biosorption processes. Also, the theoretical and experimental equilibrium biosorption capacities (q_e) differed widely for both CR and CV, confirming that biosorption of CR and CV onto HFs does not follow pseudo-first-order kinetics. On the other hand, the pseudo-second-order kinetic model shows excellent fit to the experimental kinetic data of biosorption of CR and CV by HFs at all temperatures studied. The pseudo-second-order rate constants, k_2 and q_e for biosorption of CR and CV at different temperatures as calculated from the plots of t/q_t versus t (figures not shown) and the

Table 1. Isotherm constants for biosorption of CR and CV by HFs at different temperatures

Dye	T (K)	Langmuir			Freundlich			Dubinin-Radushkevich			
		q_m (mg g^{-1})	K_L (l mg^{-1})	R^2	K_F (mg g^{-1}) (l $mg^{-1})^{1/n}$	n	R^2	q_m (mg g^{-1})	β ($mmol^2$ J^{-2})	E (kJ mol^{-1})	R^2
CR	293	72.17	1.487	0.998	14.90	2.56	0.943	56.98	4.38×10^{-9}	10.67	0.902
	303	75.29	1.732	0.997	19.12	2.97	0.952	59.41	4.12×10^{-9}	11.01	0.908
	313	78.62	1.896	0.994	22.71	3.24	0.948	62.86	3.89×10^{-9}	11.33	0.912
CV	293	55.23	0.722	0.998	26.40	5.83	0.947	37.27	2.75×10^{-9}	13.47	0.926
	303	58.76	0.945	0.995	29.19	6.39	0.955	40.14	2.43×10^{-9}	14.33	0.911
	313	63.49	1.093	0.992	31.68	6.76	0.941	42.53	2.13×10^{-9}	15.29	0.918

Table 2. Kinetic parameters for biosorption of CR and CV by HFs

Dye	T (K)	$q_{e,exp}$ (mg g^{-1})	Pseudo-first-order			Pseudo-second-order		
			$q_{e,cal}$ (mg g^{-1})	k_1 (min^{-1})	R^2	$q_{e,cal}$ (mg g^{-1})	k_2 (g mg^{-1} min^{-1})	R^2
CR	293	69.24	41.73	6.34×10^{-2}	0.796	70.12	1.46×10^{-3}	0.992
	303	72.66	44.25	7.10×10^{-2}	0.813	73.89	3.51×10^{-3}	0.997
	313	74.17	47.03	8.85×10^{-2}	0.762	74.92	6.29×10^{-3}	0.996
CV	293	53.91	27.83	1.50×10^{-3}	0.849	54.73	2.76×10^{-4}	0.998
	303	57.35	30.64	2.62×10^{-2}	0.872	58.17	5.62×10^{-4}	0.998
	313	60.29	33.57	3.49×10^{-2}	0.821	61.02	9.81×10^{-4}	0.999

corresponding correlation coefficients values are given in Table 2. All the correlation coefficients at different temperatures for both the dyes are considerably high (R^2>0.99). In addition the theoretical q_e values show good agreement with the experimental q_e values for both CR and CV, confirming that the ongoing biosorption processes proceed via a pseudo-second-order mechanism involving sharing or exchange of electrons between the dyes and the biosorbent. Similar results have been reported in the literature for biosorption of CR by bentonite [38] and CV by NaOH-modified rice husk [2].

In a well-agitated batch biosorption system, there is a possibility of intraparticle pore diffusion of adsorbate ions, which can be the rate-limiting step. Therefore, the possibility of intra-particle diffusion resistance affecting the biosorption process was explored by using the intra-particle diffusion model [37].

$$\text{Intraparticle diffusion: } q_t = k_i t^{0.5} \tag{9}$$

According to Eq. (9), if a plot of q_t versus $t^{0.5}$ is linear and passes through the origin, then intraparticle diffusion is the sole rate-limiting step. In the present study, the plots of q_t versus $t^{0.5}$ were linear at all temperatures for both CR and CV, but the plots did not pass through the origin (figure not shown), suggesting that though intraparticle diffusion was involved in the biosorption processes, it was not the only rate-controlling step and that some other mechanisms also play an important role.

2-6. Activation Energy

The activation energies (E_a) of CR and CV biosorption processes by HFs was determined using the Arrhenius equation [1]:

$$\ln k = \ln A - \frac{E_a}{RT} \tag{10}$$

E_a was obtained from the slope of the linear plots of $\ln k_2$ versus 1/T and were calculated as 55.95 kJ mol^{-1} and 48.53 kJ mol^{-1} for CR and CV, respectively. According to the literature [1], these values suggest that biosorption of both CR and CV onto HFs proceeds via a chemical-ion exchange mechanism as already inferred from the D-R isotherm.

2-7. Biosorption Thermodynamics

Thermodynamic parameters, namely Gibbs free energy change (ΔG^0), enthalpy (ΔH^0) and entropy (ΔS^0), for the CR-HFs and CV-HFs systems were calculated using the following equations for the temperature range 293-313 K [1]:

$$\Delta G^0 = -RT \ln K_C \tag{11}$$

$$K_C = \frac{C_a}{C_e} \tag{12}$$

Table 3. Thermodynamic parameters for biosorption of CR and CV by HFs

Dye	T (K)	ΔG^0 (kJ mol^{-1})	ΔH^0 (kJ mol^{-1})	ΔS^0 (J mol^{-1} K^{-1})
CR	293	−16.87	46.73	182.00
	303	−18.31		
	313	−20.52		
CV	293	−12.38	28.48	139.00
	303	−13.81		
	313	−15.17		

$$\Delta G^0 = \Delta H^0 - T\Delta S^0 \tag{13}$$

The calculated ΔG^0 values for biosorption of CR and CV onto HFs at all temperatures are listed in Table 3, as are the values of ΔH^0 and ΔS^0 as determined from the slope and intercept of the plots of ΔG^0 versus T. Negative values of ΔG^0 indicate the thermodynamically feasible and spontaneous nature of the dye biosorption processes. Positive values of ΔH^0, 46.73 kJ mol^{-1} and 28.48 kJ mol^{-1} for CR and CV, respectively, imply that the biosorption phenomena are endothermic. In addition positive ΔS^0 values for both CR-HFs and CV-HFs systems reflects the affinity of the biosorbent towards the sorbate species. It also suggests increased randomness at the solid/solution interface [39].

3. Column Studies

To evaluate the effectiveness of HFs for continuous mode dye biosorption, column experiments were performed. The effects of feed flow rate and bed height were studied.

3-1. Effect of Feed Flow Rate

Flow rate is an important parameter in evaluating the performance of a biosorption process, particularly for continuous treatment of wastewater on industrial scale. Therefore, the effect of flow rate on the CR and CV biosorption characteristics of HFs in the continuous flow packed bed column was examined by varying the flow rate from 5 to 15 mL min^{-1}, while the bed height and initial dye concentration was kept constant at 5 cm and at 50 mg L^{-1}, respectively. The effect of flow rate on breakthrough performance at the above operating conditions is shown in Fig. 6(a)-(b). It can be seen that the biosorption of each dye onto HFs is strongly dependent on flow rate. In general, for both the dyes, the breakthrough curves become stepper and breakthrough time decreases with increasing flow rate. This can be explained by the fact that at lower flow rate, the residence time of the dye ions is more and hence they get more time to capture the available reaction sites of the biosorbent [40]. The dye ions also

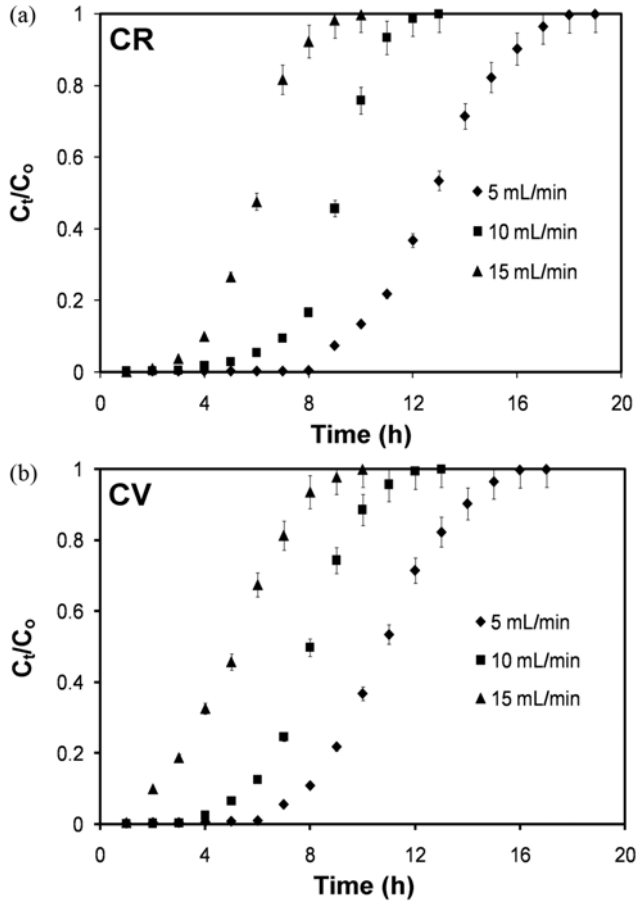

Fig. 6. Effect of flow rate on breakthrough curve for biosorption of CR and CV onto HFs (h=5 cm; C_0=50 mg L^{-1}).

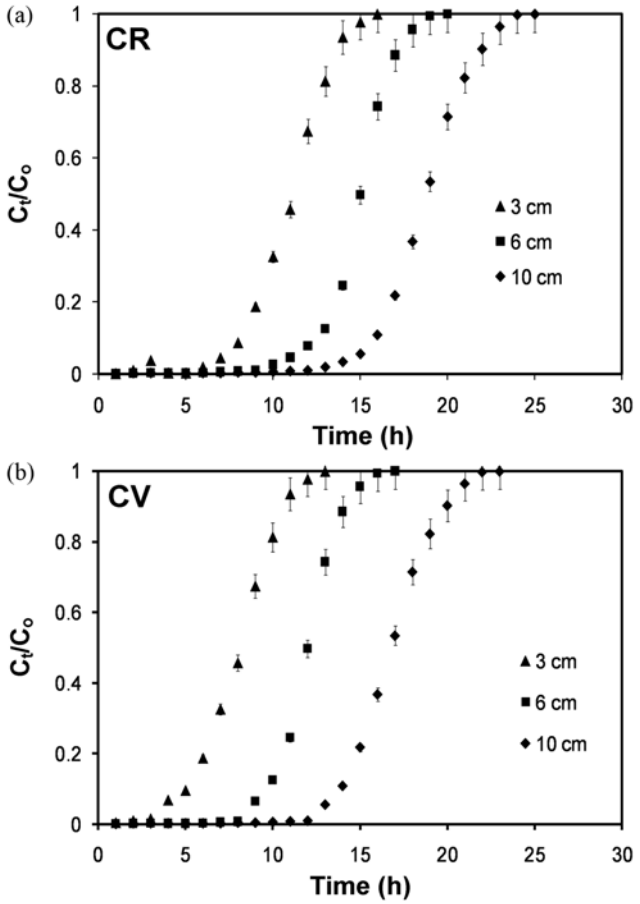

Fig. 7. Effect of bed height on breakthrough curve for biosorption of CR and CV onto HFs (v=5.0 mL min^{-1}; C_0=50 mg L^{-1}).

have more time to diffuse into the pores of the biosorbent through intra-particle diffusion. As the flow rate increases, the residence time of the dye solution in the column decreases. The contact time of the dye ions with the biosorbent is very short and hence they do not have enough time to capture the reaction sites on the biosorbent surface or diffuse into the pores of the biosorbent, leaving the column before equilibrium occurs [41].

3-2. Effect of Bed Height

The column biosorption performance of HFs for CR and CV dyes was also tested at different bed heights. For this purpose a dye solution having influent concentration 50 mg L^{-1} was passed through the column at a flow rate of 5.0 mL min^{-1} by varying the bed height from 3 to 10 cm. Fig. 7(a)-(b) represents the performance of breakthrough curves at bed heights of 3 cm, 6 cm, and 10 cm. From Fig. 7(a)-(b), the breakthrough time increased with increasing the bed height for both CR-HFs and CV-HFs systems. As the bed height increased, the dye ions had more time to contact with HFs resulting in higher removal efficiency in the column [41]. Also, the slope of breakthrough curve decreased with increasing bed height due to an increase in the availability of more binding sites for the biosorption.

3-3. Modeling of Column Data

In this study, the bed depth service time (BDST) model and Tho-

Table 4. BDST model parameters for continuous fixed-bed biosorption of CR and CV by HFs

Parameters	CR			CV		
	k (mL mg^{-1} min^{-1})	N_o (mg L^{-1})	R^2	k (mL mg^{-1} min^{-1})	N_o (mg L^{-1})	R^2
Flow rate (mL min^{-1})						
5	0.764	18972	0.945	0.431	13782	0.929
10	0.763	17026	0.934	0.430	12257	0.927
15	0.762	16412	0.941	0.429	11366	0.934
Bed height (cm)						
3	0.562	16871	0.951	0.263	12892	0.917
6	0.461	17689	0.944	0.156	13764	0.923
10	0.343	18972	0.947	0.086	14562	0.025

Table 5. Thomas model parameters for continuous fixed-bed biosorption of CR and CV by HFs

Parameters	CR				CV			
	k_{Th} (mL mg^{-1} min^{-1})	q_o (mg g^{-1})	$q_{e,exp}$ (mg g^{-1})	R^2	k_{Th} (mL mg^{-1} min^{-1})	q_o (mg g^{-1})	$q_{e,exp}$ (mg g^{-1})	R^2
Flow rate (mL min^{-1})								
5	0.346	85.68	86.88	0.986	0.138	74.27	75.42	0.982
10	0.452	81.87	82.64	0.981	0.296	70.76	71.31	0.990
15	0.517	76.25	77.42	0.982	0.342	65.31	66.29	0.985
Bed height (cm)								
3	0.257	83.26	84.13	0.991	0.115	70.17	71.38	0.983
6	0.169	88.59	89.61	0.986	0.085	75.63	76.92	0.987
10	0.099	93.73	94.55	0.988	0.056	79.47	80.27	0.985

mas model were fitted to the dynamic flow experimental data of CR and CV in order to determine the characteristic parameters of the column [42].

$$\text{BDST: } t = \frac{N_0 Z}{C_0 u} - \frac{1}{C_0 k}\ln\left[\frac{C_0}{C_t} - 1\right] \quad (16)$$

$$\text{Thomas: } \ln\left[\left(\frac{C_0}{C_t}\right) - 1\right] = \frac{k_{Th} q_0 m}{F} - k_{Th} C_0 t_e \quad (17)$$

where N_0 is the maximum volumetric sorption capacity (mg L^{-1}), Z is the bed height (cm), C_0 is the initial dye concentration (mg L^{-1}), C_t is the concentration of dye at time t (mg L^{-1}), u is the linear velocity (cm min^{-1}), k is the biosorption rate constant (L mg^{-1} min^{-1}), k_{Th} is the Thomas rate constant (mL mg^{-1} min^{-1}), q_0 is the equilibrium adsorbate uptake (mg g^{-1}), m is the mass of the biosorbent in the column (g), F is the volumetric flow rate (mL min^{-1}) and t_e is the bed exhaustion time (min).

The BDST model parameters k and N_0 as estimated from the slope and intercept of the plot between $\ln(C_0/C_t - 1)$ versus t at different experimental conditions are presented in Table 4. The correlation coefficient (R^2) values are also given in Table 4. Analysis of the R^2 values suggests that the BDST model does not provide a good fit to the dynamic biosorption data of CR and CV. With increasing bed height, the rate constant (k) decreases while the volumetric sorption capacity of the bed (N_0) increases. Such behavior can be attributed to establishment of a greater interaction between dye and biosorbent due to prolonged residence time of the fluid inside the column at higher bed heights. Furthermore, as seen in Table 4, k did not change significantly with change in flow rate, implying that the BDST model can be used to scale up to other flow rates without further experimental tests [42].

The Thomas rate constant (k_{Th}) and bed capacity (q_0) were calculated from the slope and intercept of the plot between $\ln(C_0/C_t - 1)$ versus t at different flow rates and bed heights. The calculated values of k_{Th} and q_0 along with regression coefficients are presented in Table 5. The relatively high R^2 (>0.98) values at all the operating conditions suggests that the Thomas model was suitable for describing the column biosorption data of CR and CV by HFs. The calculated q_e values (q_o) show good agreement with the experimental q_e values ($q_{e,exp}$), further confirming the suitability of the Thomas model for column design and analysis. From Table 5, it can be seen that as the flow rate increases, the bed capacity (q_0) decreases while the Thomas rate constant (k_{Th}) increases. The Thomas model showed good agreement with the dynamic flow experimental data. On the contrary, q_o increases and k_{Th} decreases with increasing bed height.

4. Comparison of HFs with Other Sorbents

A comparative study of the maximum dye uptake capacity of HFs has been carried out with other reported sorbents. The maximum amount of CR and CV uptake by HFs has been compared to the maximum CR/CV uptake capacity of other reported sorbents and is presented in Table 6. From Table 6 it is evident that the maximum sorption capacity of HFs for CR and CV is comparable and

Table 6. Comparison of CR and CV biosorption capacity of HFs with other reported low-cost adsorbents

Sorbent	Maximum sorption capacity (mg g^{-1})	Reference
CR		
Fly ash	4.125	[43]
Acid activated red mud	7.08	[44]
Bagasse fly ash	11.89	[45]
Montmorillonite	12.70	[46]
Aspergillus niger	14.7	[47]
Orange peel	14.0	[48]
Banana peel	18.2	[48]
Jute stick powder	35.7	[49]
Cattail root	38.79	[50]
Neem leaf powder	41.20	[28]
Eggshells	69.45	[27]
Hen feathers	78.62	This study
CV		
Coir pith	2.56	[51]
Sugarcane dust	3.8	[52]
Neem sawdust	3.8	[53]
Calotropis procera leaf	4.14	[54]
Jalshakti® Polymer	12.9	[55]
Orange peel	14.3	[48]
Jute fiber carbon	27.99	[56]
Coniferous pinus bark powder	32.78	[29]
Rice bran	42.25	[57]
Jackfruit leaf powder	43.39	[42]
NaOH-modified rice husk	44.87	[2]
Hen feathers	63.49	This study

moderately higher than that of many corresponding sorbent materials. Differences in dye uptake capacity are due to the properties of each sorbent material such as structure, functional groups and surface area. The easy availability and cost effectiveness of HFs are some additional advantages, which make it better biosorbent for treatment of dye effluents.

CONCLUSION

The use of HFs was investigated as a low-cost biosorbent for removal of CR and CV from aqueous solutions. Batch biosorption experiments were conducted in order to evaluate the effect of operational parameters - solution pH, initial dye concentration and temperature on the dye uptake performance of the biosorbent. Both CR and CV biosorption processes were found to be highly dependent on reaction temperature and solution pH. The equilibrium biosorption data of both CR and CV fitted well in the Langmuir isotherm model, indicating monolayer sorption on a homogeneous surface. The maximum monolayer uptakes were 78.62 mg g^{-1} for CR and 63.49 mg g^{-1} for CV at 313 K. Kinetic studies showed that the biosorption of CR and CV onto HFs followed pseudo-second order kinetics. Activation energy values further confirmed that the biosorption mechanism involved chemical ion-exchange. Thermodynamic studies showed that biosorption of CR and CV was spontaneous and endothermic. To evaluate the effectiveness of HFs for continuous mode dye biosorption, packed-bed column experiments were also performed. The column breakthrough curves were analyzed at different feed flow rate and bed height. Breakthrough time increased with increase in bed height but decreased with increase in flow rate. The results suggest that HFs is a promising biosorbent for decoloration of dye bearing effluents.

NOMENCLATURE

A : arrhenius constant
C_a : equilibrium dye concentration on the biosorbent [mg l^{-1}]
C_e : equilibrium dye concentration in solution [mg l^{-1}]
C_i : initial dye concentration [mg l^{-1}]
C_o : influent dye concentration [mg l^{-1}]
C_t : effluent dye concentration [mg l^{-1}]
E : mean free energy [kJ mol^{-1}]
E_a : activation energy [kJ mol^{-1}]
ΔG^0 : gibbs free energy change [kJ mol^{-1}]
ΔH^0 : enthalpy of reaction [kJ mol^{-1}]
h : bed height [cm]
K_C : distribution coefficient for biosorption
K_F : freundlich constant [mg g^{-1}] [l g^{-1}]$^{1/n}$
K_L : langmuir constant [l mg^{-1}]
k : rate constant
k_i : intraparticle diffusion rate constant [mg $g^{-1}min^{-0.5}$]
k_1 : pseudo-first-order rate constant [min^{-1}]
k_2 : pseudo-second-order rate constant [g mg^{-1} min^{-1}]
m : mass of biosorbent [g]
n : freundlich adsorption isotherm constant
q_e : equilibrium dye concentration on biosorbent [mg g^{-1}]
q_m : maximum biosorption capacity [mg g^{-1}]
q_t : amount of dye adsorbed at time t [mg g^{-1}]
R : universal gas constant [8.314 J $mol^{-1}K^{-1}$]
R^2 : correlation coefficient
ΔS^0 : entropy of reaction [J mol^{-1} K^{-1}]
T : temperature [K]
V : volume of the solution [l]
v : feed flow rate [mL min^{-1}]

Greek Alphabet

β : D-R isotherm constant [$mmol^2$ J^{-2}]
ε : polanyi potential [J $mmol^{-1}$]=RT ln(1+1/C_e)

REFERENCES

1. P. Saha, S. Chowdhury, S. Gupta and I. Kumar, *Chem. Eng. J.*, **165**, 874 (2010).
2. S. Chakraborty, S. Chowdhury and P. D. Saha, *Carbohydr. Polym.*, **86**, 1533 (2011).
3. M. Asgher and H. N. Bhatti, *Ecol. Eng.*, **36**, 1660 (2010).
4. Y. Safa and H. N. Bhatti, *Desalination*, **272**, 313 (2011).
5. I. Haq, H. N. Bhatti and M. Asgher, *Can. J. Chem. Eng.*, **89**, 593 (2011).
6. S. Chowdhury, R. Mishra, P. Saha and P. Kushwaha, *Desalination*, **265**, 159 (2011).
7. Y. Safa and H. N. Bhatti, *Chem. Eng. J.*, **167**, 35 (2011).
8. H. N. Bhatti, N. Akhtar and N. Saleem, *Arab. J. Sci. Eng.*, **37**, 9 (2012).
9. S. Chowdhury, S. Chakraborty and P. Saha, *Colloids Surf. B.*, **84**, 520 (2011).
10. B. H. Hameed and M. I. El-Khaiary, *J. Hazard. Mater.*, **153**, 701 (2008).
11. R. Malik, D. S. Ramteke and S. R. Wate, *Waste Manage.*, **27**, 1129 (2009).
12. P. Saha, *Water Air Soil Pollut.*, **213**, 287 (2010).
13. Y. Bulut and H. Aydin, *Desalination*, **194**, 259 (2006).
14. M. T. Sulak, E. Demribas and M. Kobya, *Bioresour. Technol.*, **98**, 2590 (2007).
15. M. Arami, N. Y. Limaee, N. M. Mahmoodi and N. S. Tabrizi, *J. Colloid Interface Sci.*, **288**, 371 (2005).
16. K. V. Kumar and K. Porkodi, *J. Hazard. Mater.*, **138**, 633 (2006).
17. B. H. Hameed, R. R. Krishna and S. A. Sata, *J. Hazard. Mater.*, **162**, 305 (2009).
18. N. Nasuha, B. H. Hameed and A. T. M. Din, *J. Hazard. Mater.*, **175**, 126 (2010).
19. V. K. Gupta, A. Mittal, A. Malviya and J. Mittal, *J. Colloid Interface Sci.*, **335**, 24 (2009).
20. S. Chowdhury and P. Saha, *J. Environ. Eng.*, **137**, 388 (2011).
21. S. Agrahari and N. Wadhwa, *Int. J. Poult. Sci.*, **9**, 482 (2010).
22. A. Aguayo-Villarreal, A. Bonilla-Petriciolet, V. Hernandez-Montoya, M. A. Montes-Moran and H. E. Reynel-Avila, *Chem. Eng. J.*, **167**, 67 (2011).
23. A. Mittal, *J. Hazard. Mater.*, **133**, 196 (2006).
24. A. Mittal, *J. Hazard. Mater.*, **128**, 233 (2006).
25. A. Mittal, L. Kurup and J. Mittal, *J. Hazard. Mater.*, **146**, 243 (2007).
26. V. K. Gupta, A. Mittal, L. Kurup and J. Mittal, *J. Colloid Interface Sci.*, **304**, 52 (2006).
27. P. D. Saha, S. Chowdhury, M. Mondal and K. Sinha, *Sep. Sci. Technol.*, **47**, 112 (2012).

28. G. Bhattacharya and A. Sharma, *J. Environ. Manage.*, **71**, 217 (2004).
29. R. Ahmad, *J. Hazard. Mater.*, **171**, 767 (2009).
30. S. Chowdhury and P. Das, *Environ. Prog. Sustainable Energy*, DOI: 10.1002/ep.10564.
31. L. Lian, L. Guo and A. Wang, *Desalination*, **249**, 791 (2009).
32. R. Kumar and R. Ahmad, *Desalination*, **265**, 112 (2011).
33. S. Chowdhury and P. Saha, *Chem. Eng. J.*, **164**, 168 (2010).
34. R. Han, J. Zhang, P. Han, Y. Wang, Z. Zhao and M. Tang, *Chem. Eng. J.*, **145**, 496 (2009).
35. V. Vimonses, S. Lei, B. Jin, C. W. K. Chow and C. Saint, *Chem. Eng. J.*, **148**, 354 (2009).
36. A. Saeed, M. Sharif and M. Iqbal, *J. Hazard. Mater.*, **179**, 564 (2010).
37. S. Chowdhury and P. Saha, *Sep. Sci. Technol.*, **46**, 1966 (2011).
38. E. Bulut, M. Ozacar and I. A. Sengil, *J. Hazard. Mater.*, **154**, 613 (2008).
39. Y. Liu and Y.-J. Liu, *Sep. Purif. Technol.*, **61**, 229 (2008).
40. V. Vinodini and N. Das, *Desalination*, **264**, 9 (2010).
41. A. A. Ahmad and B. H. Hameed, *J. Hazard. Mater.*, **175**, 298 (2010).
42. P. D. Saha, S. Chakraborty and S. Chowdhury, *Colloids Surf. B.*, **92**, 262 (2012).
43. V. V. Rao and S. R. M. Rao, *Chem. Eng. J.*, **116**, 77 (2006).
44. A. Tor and Y. Cengeloglu, *J. Hazard. Mater.*, **138**, 409 (2006).
45. I. D. Mall, V. C. Srivastava, N. K. Agarwal and I. M. Mishra, *Chemosphere*, **61**, 492 (2005).
46. L. Wang and A. Wang, *J. Hazard. Mater.*, **147**, 979 (2007).
47. Y. Fu and T. Viraraghavan, *Adv. Environ. Res.*, **7**, 239 (2007).
48. G. Annadurai, R.-S. Juang and D.-J. Lee, *J. Hazard. Mater.*, **92**, 263 (2004).
49. G. C. Panda, S. K. Das and A. K. Guha, *J. Hazard. Mater.*, **164**, 374 (2009).
50. Z. Hua, H. Chen, F. Ji and S. Yuan, *J. Hazard. Mater.*, **173**, 292 (2010).
51. C. Namasivayam, M. D. Kumar, K. Selkvi, R. A. Begum, T. Vanathi and R. T. Yamuna, *Biomass Bioenergy*, **6**, 477 (2001).
52. S. D. Khattri and M. K. Singh, *Adsorpt. Sci. Technol.*, **17**, 269 (1999).
53. S. D. Khattri and M. K. Singh, *Water Air Soil Pollut.*, **120**, 283 (2009).
54. H. Ali and S. K. Muhammad, *J. Environ. Sci. Technol.*, **1**, 143 (2008).
55. R. Dhodapkar, N. N. Rao, S. P. Pande, T. Nandy and S. Devotta, *React. Funct. Polym.*, **67**, 540 (2007).
56. K. Porkodi and K. V. Kumar, *J. Hazard. Mater.*, **143**, 311 (2007).
57. X. S. Wang, X. Liu, L. Wen, Y. Zhou and Z. Li, *Sep. Sci. Technol.*, **43**, 3712 (2008).